High-sensitivity ultrasound detection based on phase-shifted fiber Bragg grating

Mingrui Xu[1,a], Jingjing Guo[1,b] and Changxi Yang[1,c]

[1]State Key Laboratory of Precision Measurement Technology and Instruments, Department of Precision Instruments, Tsinghua University, Beijing, China

[a]mrxu1234@yahoo.cn, [b]1278630522@qq.com, [c]cxyang@tsinghua.edu.cn

Keywords: ultrasound detection; phase-shifted fiber Bragg grating; LabVIEW; high sensitivity

Abstract. Fiber Bragg grating based ultrasound sensors has been receiving continuous attention from science and industry. It is of great potential in medical imaging, oil exploration, etc. In this paper, we construct an all fiber ultrasound sensing system with cascaded phase-shifted FBG and a normal FBG. Correlation algorithm is used to improve the detection sensitivity based on data acquisition board and virtual instrument LabVIEW. In the experiment, the system sensitivity is calculated as $9n\varepsilon/\sqrt{Hz}$ and the dynamic range of the system is 79.33dB.

Introduction

Since fiber Bragg grating (FBG) was first used as strain and temperature sensors in 1989[1], it has made continuous and fast progress during the two decades. FBG sensors have many advantages over their counterparts such as small size, immunity to electromagnetic interference, and wide bandwidth etc. FBG sensors are now widely used in many industries, such as aerospace, civil engineering, composite material, petrochemical engineering and so on[2]. With fast progress in other disciplines and the background of trans-discipline, FBG sensors are gradually found that can be used to detect ultrasound, in place of traditional piezoe-lectric transducer (PZT) sensors[3]. Further, FBG sensors can be developed and used as hydrophones, in structure health monitoring system, ultrasound distance measurement system, etc[4-6]. FBG based ultrasound sensors have great potential to industrial application.

For all types of ultrasound sensors, weak signal detection remains a difficult issue, for the ultrasound signal generally appears at a very low amplitude along with noises from each system node, which could now and then submerge the desired signal and hinder useful data extraction. Meanwhile, the ultrasound signal usually has a large bandwidth, from 20kHz to 1MHz of the acoustic emission at the appearance of damage. Therefore, broad bandwidth is necessary in the ultrasound sensing system. Besides, large dynamic range is also needed for distributed detecting system for the amplitude of the signal from the nearest point to the signal from the farthest point has a large magnitude difference. The earlier researches focused on the bandwidth scope of the FBG, which resulted that the upper detection frequency limit was decided by the fiber length of the FBG[7-9]. Later, researchers began to pay attention to the resolution and then got a high sensitivity system[10]. However, most present detection systems do not mention the dynamic range, especially for high sensitivity system. How to improve the dynamic range of the system while keeping high sensitivity is of great significance for industrial application.

In this paper, we use a phase-shifted fiber Bragg grating (PS-FBG) cascaded with a normal FBG to guarantee both the high sensitivity and large dynamic range of the system. Meanwhile, we use a balanced photo detector to eliminate the laser intensity noise[10]. For the acquisition part, we built a compact correlation detection system, simply comprised of data acquisition (DAQ) board NI USB-6366 and virtual instrument LabVIEW. Correlation calculation is performed in LabVIEW, so we do not have to adopt discrete hardware circuitries[11]. As for practical use, we applied this detection system for detecting the ultrasound on the aluminium plate, and compare with PZT

transducer. The result indicates that the system sensitivity limit is better than $10n\varepsilon/\sqrt{Hz}$ and the dynamic range is around 80dB.

Theory of the system and Experimental configuration

A. System hardware structure**.** Fig. 1 shows the system schematic diagram. The tunable laser Agilent 8164 is used as a light source with a linewidth of 100kHz and the tunable resolution is 0.1pm. The circulator connects the laser and the cascaded FBG and phase-shifted FBG with port 1 and port 2, respectively. The transmitted light and the reflected light are input into two ports of the balanced photo detector (KG-BPR-200M). The BPD contains two PDs and two amplifiers with the gain of 2×10^4. The converted electric signal is input into the DAQ card USB-6366, and further into PC to deal with. The FBG and PS-FBG are glued on the $250\times250\times2mm^3$ aluminum plate. PZT 1 and PZT 2 are placed on the plate with the acoustic couplant. The distance from PS-FBG to PZT 1 and PZT 2 to PZT 1 is the same, 5cm. A function generator (FG) is used to generate waves with different peak-to-peak voltages and frequencies to drive the PZT actuator, PZT 1. PZT 2 is used to detect ultrasound, comparing the performance with PS-FBG.

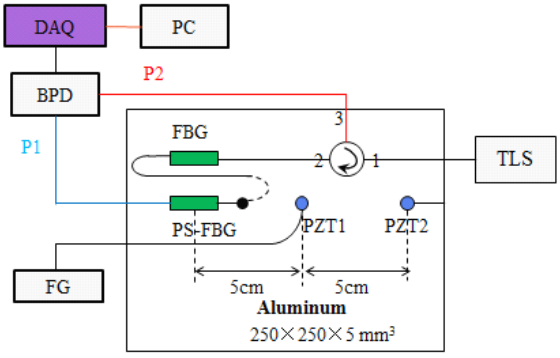

Fig. 1 System configuration

B. Theory of the system. The demodulation method of the system is edge filter detection, as is shown in Fig. 2. The wavelength of the narrow linewidth TLS is set around the 3dB location of the PS-FBG or FBG spectrum, where the reflectivity and the transmittance are around 0.5. If there is no ultrasound signal, the reflected signal into one port of the BPD is the same as the transmitted signal into another port of the BPD. The two signals subtract and are amplified in the BPD, so the output voltage is 0V. When the PS-FBG or FBG has detected the ultrasound signal, the two input signals from the two ports of the BPD have the same amplitude but the opposite phase because of the sensing principle of the FBG[12] . Therefore we can detect the AC voltage from the BPD to demodulate the ultrasound signal. In this system, the linear region of the FBG and PS-FBG is used. Fig. 3 show the spectrum of the PS-FBG we used in this experiment.

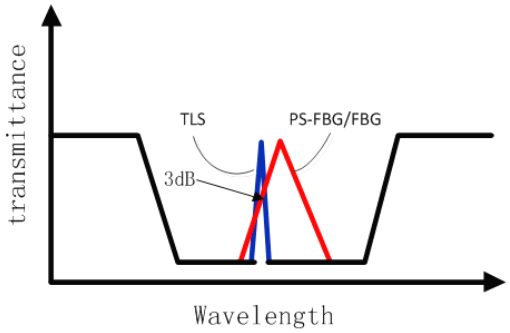

Fig. 2 System demodulation principle

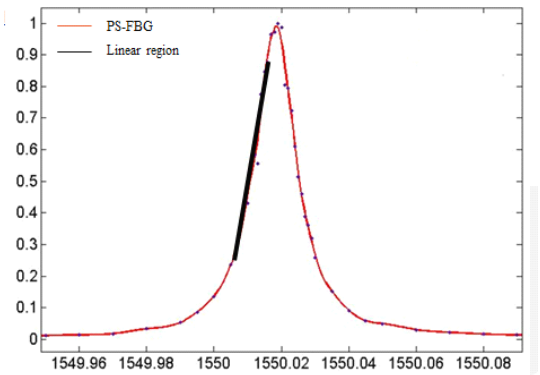

Fig. 3 Tested PS-FBG spectrum

The PS-FBG used in this system is the key component to guarantee the high sensitivity. PS-FBG is one kind of aperiodic FBG, which open one or several extremely narrow transmission window in the

reflectivity spectrum[13,14], as is shown in Fig. 4. The bandwidth of the PS-FBG is only about 0.016nm, which is only tenths of a normal FBG. In the experiment, the bandwidth of the FBG we used is 0.2nm.

The linear slope rate of the PS-FBG is 70nm^{-1}, which is 140 times in comparison with the normal FBG of 0.5nm^{-1}. This means that weak ultrasound signal can generate much larger amplitude of the AC voltages due to the edge filter detection principle. Meanwhile, in order to maintain a relatively large dynamic range, a normal FBG is cascaded. The system can work in two states due to different central wavelengths of the FBG and PS-FBG: the high sensitivity mode and the large dynamic range mode. The function of the BPD is to eliminate the large DC voltage and the laser intensity noise.

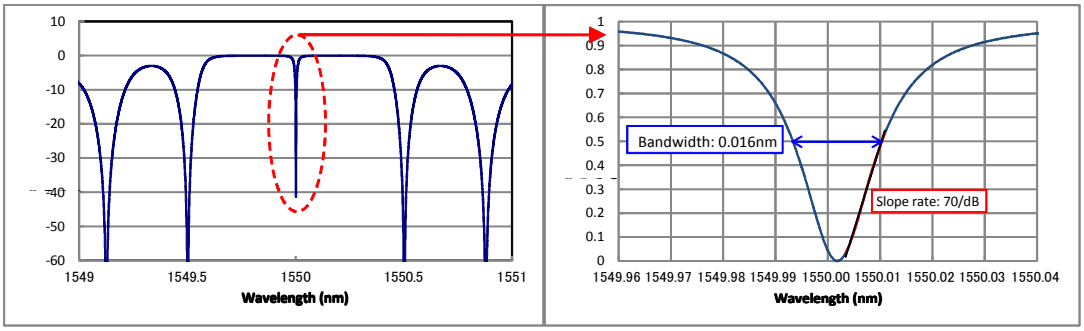

Fig. 4 PS-FBG property and spectrum diagram

The voltage we get from the system can be written as follows. $\Delta\lambda_s$ represents the wavelength shift of the PS-FBG or FBG, S is the slope rate of the grating, P_D means the the PD's response factor, I is the input light power and g means the gain of the BPD.

$$V_{AC} = 2\Delta\lambda_s SP_D Ig \tag{1}$$

The sensitivity of the system can be regarded as the minimum voltage that can be detected, which means the desired signal is the same magnitude with the system noise V_N. Then the sensitivity can be written as formula (3).

$$V_N = V_{AC} \tag{2}$$

$$\Delta\lambda_{s\min} = \frac{V_{AC}}{2SP_D Ig} \tag{3}$$

C. Principle of the correlation detection based on LabVIEW. Correlation function method is widely used in the weak signal detection field. It is based on the correlation of the measured periodical signal formerly and latterly. As an effective indicator of this relevance, correlation function can be utilized to extract the desired signal deeply buried in noise. According to the number of signals involved in calculation, correlation is categorized into autocorrelation and cross-correlation, in which the latter is more widely used for its better noise immunity and to be used in this paper. The cross-correlation function can be written as follows:

$$\begin{aligned} R_{xr}(\tau) &= \lim_{T\to\infty}[\frac{1}{T}\int_{-T/2}^{T/2} x(t)r(t-\tau)dt] \\ &= \lim_{T\to\infty}[\frac{1}{T}\int_{-T/2}^{T/2} s(t)r(t-\tau)dt + \int_{-T/2}^{T/2} n(t)r(t-\tau)] \\ &= R_{sr}(\tau) + R_{nr}(\tau) \\ & r(t) \end{aligned} \tag{4}$$

In the function, $x(t)$ represents the input signal, which concludes the desired signal $s(t)$ and the noise $n(t)$. Because the noise is uncorrelated to the local reference signal $r(t)$, their correlation result $R_{nr}(\tau)$ equals zero. Therefore, we can extract the desired signal from the correlation function $R_{sr}(\tau)$.

We use this function in the distance measurement experiment based on LabVIEW, a well developed graphical software system. It contains powerful signal processing modules and is widely used in high-performance scientific and engineering applications development. LabVIEW itself has the correlation function which is realized by Fast Fourier Transform Algorithm, as is shown in Fig. 5. x(n) serves as the input signal and y(n) serves as the local reference signal. The algorithm first calculate their Fourier transforms X(k) and Y(k), then multiply Y(k) by the conjugate of X(k). Then the cross-correlation result is get through the inverse FFT. This algorithm of function can work fast and deal with high data volume situation.

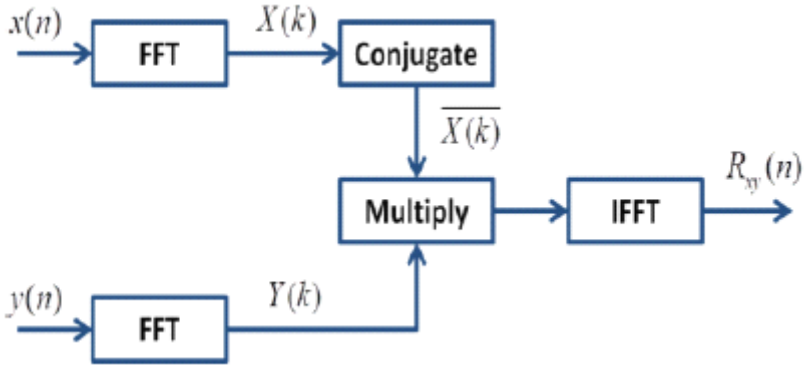

Fig. 5 FFT Algorithm of the correlation function

The final distance measurement program is shown in Fig. 6. The local reference signal is generated by the function generator and is collected by one analog input channel of the DAQ card. As the system is working, when the DAQ card has detected the local signal, the interval timer begins to work. The cross-correlation signal is sent to the peak-search module after denoising, where we get the travelling time of the ultrasound and finally calculate the distance after multiplying the wave speed.

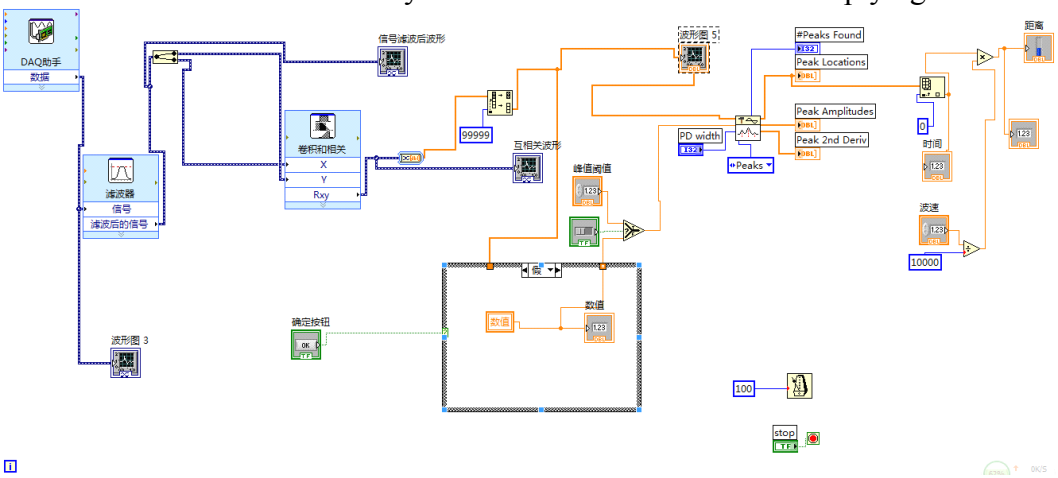

Fig. 6 Block diagram of correlation detection system

Fig. 7 shows the virtual instrument front panel of the distance measurement system when it is working. The waveforms show the collected signals, cross-correlation signal and denoising signal. The cylinder on the left side shows the real time distance between the PS-FBG and the PZT actuator.

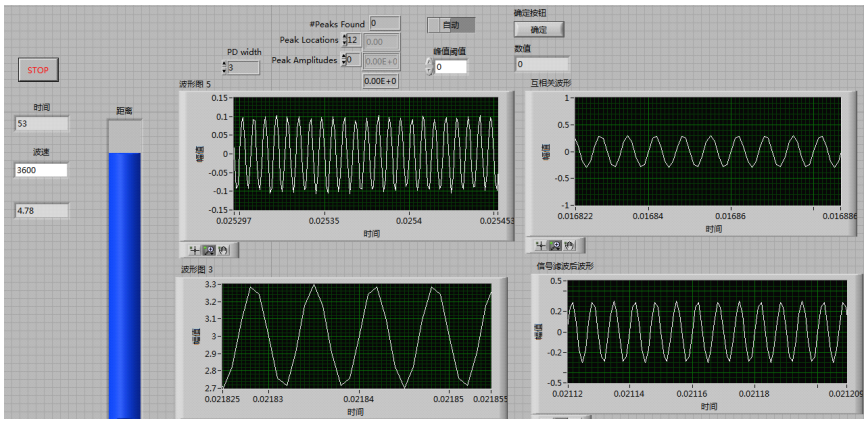

Fig. 7 Front panel of the distance measurement system

Results and discussion

System sensitivity and dynamic range**.** In order to test the performance of the system, the function generator is used to generate sinusoidal wave and sinusoidal burst wave with different peak-to-peak voltages and frequencies to drive PZT 1. Fig. 8 shows the frequency-domain plot of the ultrasound generated by different peak-to-peak voltages with the frequency of 150 kHz.

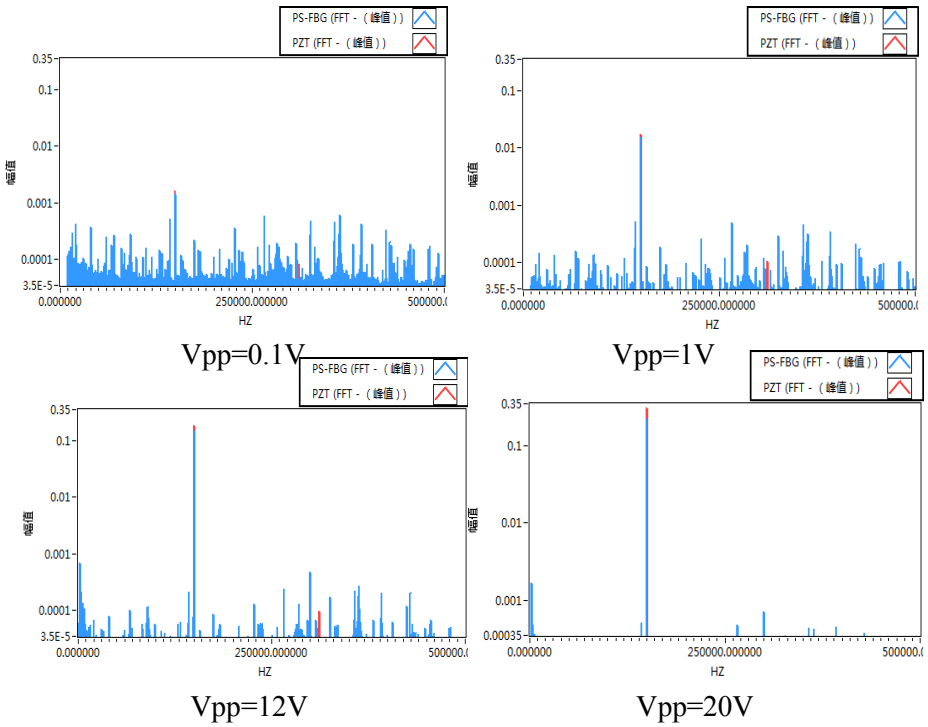

Fig. 8 FD plot of the detected ultrasound signal by PS-FBG and PZT 2

Fig. 8 indicates that we can regard the minimum voltage that can be detected is 0.1V. The central wavelength of the PS-FBG in this experiment is 1550. 0198nm, the linewidth is 0.018nm, and the calculated grating slope is 78nm^{-1}. According to the formula $\Delta\lambda_s = \alpha\varepsilon$, as $\alpha = 1.2pm/\mu\varepsilon$ around 1550nm for FBG, we can get the sensitivity of the system from formula (3). The corresponding minimum detected sensitivity is calculated as, $9n\varepsilon/\sqrt{Hz}$.

Table 1 shows the comparison result between PS-FBG and PZT with different ultrasound frequencies. The peak-to-peak voltage of the function generator is 20V. From Table 1, it shows that PS-FBG has a broader frequency response than PZT. The detection amplitude is similar only around 100kHz to 200kHz, while at the low frequency and high frequency, there is big difference between them. The 150kHz is the resonant frequency of the PZT.

Table 1 Comparison result of PS-FBG and PZT

Ultrasound frequency（kHz）	**50**	**100**	**150**	**200**	**300**	**500**	**800**
PS-FBG output（V）	0.09	0.09	0.18	0.08	0.04	0.035	0.02
PZT output（V）	0.01	0.07	0.23	0.07	0.005	0.0008	0.0005

The dynamic range of the system can be defined as (5):

$$D = 20\lg(\frac{\varepsilon_{\max}}{\varepsilon_{\min}}) \tag{5}$$

The $\varepsilon_{\min} = 9n\varepsilon / \sqrt{Hz}$, which is the system sensitivity. The $\varepsilon_{\max}$ means the max strain that can be detected in the linear sensing region of the PS-FBG and FBG, which can be approximately written as :

$$\varepsilon_{\max} = \frac{Linewidth}{2\alpha} \tag{6}$$

If there is no normal FBG in the system, then (6) can be written as (7):

$$\varepsilon_{\max} = \frac{Linewidth_{PS-FBG}}{2\alpha} \tag{7}$$

From (5) and (7), the calculation result is $D = 58.42dB$. Consider this cascaded system, (7) can be changed as (8):

$$\varepsilon_{\max} = \frac{Linewidth_{FBG}}{2\alpha} \tag{8}$$

The dynamic range is $D = 79.33dB$.

Conclusion

We construct a compact PS-FBG based ultrasound detection system by utilization of DAQ board and LabVIEW, and apply it into distance measurement. Experimental results show that the sensitivity limit is $9n\varepsilon / \sqrt{Hz}$, with the dynamic range of 79.33dB.

References

[1] W.W. Morey, G. Meltz, W.H. Glenn. Fiber Optic Bragg grating sensors Proc. SPIE, 1989

[2] Willsch R. Application of optical fiber sensors: technical and market trends[C]//Symposium on Applied Photonics. International Society for Optics and Photonics, 2000: 24-31.

[3] D. J.Webb et al. Miniature fiber optic ultrasonic probe. Proc. SPIE,vol. 2839, 1996: 76-80

[4] N. Takahashi, A. Hirose, and S. Takahashi, Underwater acoustic sensor with fiber Bragg grating, Opt. Rev., 1997,4(6): 691–694.

[5] N. Takahashi, K. Yoshimura, and S. Takahashi, Fiber Bragg grating vibration sensor using incoherent light, Jpn. J. Appl. Phys., 2001, 40(5b): 3632-3636.

[6] N.Takahashi, K.Yoshimura, and S.Takahashi, FBG vibration sensor based on intensity-modulation method with incoherent light, Proc. SPIE, 2001, 4416(62-65).

[7] N. E. Fisher et al., Ultrasonic field and temperature sensor based on short in-fiber Bragg gratings. Electron. Lett., 1998, 34(11): 1139-1140,.

[8] N. E. Fisher et al., Ultrasonic hydrophone based on short in-fiber Bragg gratings. Appl. Opt., 1998, 37(34): 8120-8128,.

[9] S. F. O'Neill et al., High-frequency ultrasound detection using a fiber Bragg grating. IEE Colloquium on Optical Fiber Gratings, 1999: 16/1-16/6.

[10] Wu Q, Okabe Y. High-sensitivity ultrasonic phase-shifted fiber Bragg grating balanced sensing system[J]. Optics express, 2012, 20(27): 28353-28362.

[11] Yanju Wang, Yutian Wang, Zhongdong Wang, "Design on Faint Signal Processing Circuit for Difference Absorption Gas Sensor," Transducer and Microsystem Technologies, Vol. 25, No. 6, pp. 1-4, 2006.

[12] Hill K O, Meltz G. Fiber Bragg grating technology fundamentals and overview[J]. Lightwave Technology, Journal of, 1997, 15(8): 1263-1276.

[13] Agrawal G P, Radic S. Phase-shifted fiber Bragg gratings and their application for wavelength demultiplexing[J]. Photonics Technology Letters, IEEE, 1994, 6(8): 995-997.

[14] Rosenthal, A., D. Razansky, et al., High-sensitivity compact ultrasonic detector based on a pi-phase-shifted fiber Bragg grating. Optics letters, 2011, 36(10): 1833-1835.